JACS
JOURNAL OF THE AMERICAN CHEMICAL SOCIETY

pubs.acs.org/JACS

Article

Enantioselective Construction of Tertiary Fluoride Stereocenters by Organocatalytic Fluorocyclization

Qiang Wang,[§] Marvin Lübcke,[§] Maria Biosca,[§] Martin Hedberg, Lars Eriksson, Fahmi Himo,* and Kálmán J. Szabó*

Cite This: *J. Am. Chem. Soc.* 2020, 142, 20048−20057

Read Online

ACCESS | Metrics & More | Article Recommendations | Supporting Information

ABSTRACT: 1,1-Disubstituted styrenes with internal oxygen and nitrogen nucleophiles undergo oxidative fluorocyclization reactions with *in situ* generated chiral iodine(III)-catalysts. The resulting fluorinated tetrahydrofurans and pyrrolidines contain a tertiary carbon−fluorine stereocenter. Application of a new 1-naphthyllactic acid-based iodine(III)-catalyst allows the control of tertiary carbon−fluorine stereocenters with up to 96% ee. Density functional theory calculations are performed to investigate the details of the mechanism and the factors governing the stereoselectivity of the reaction.

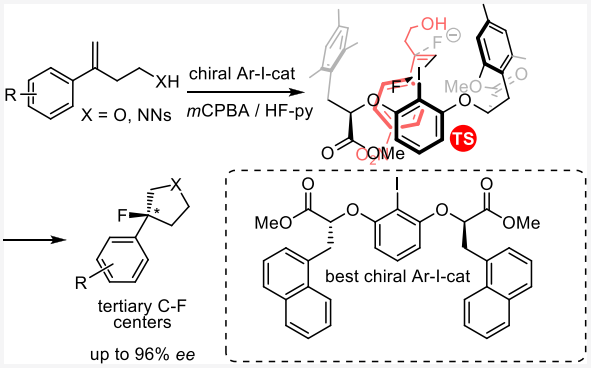

INTRODUCTION

Carbon−fluorine bonds frequently occur in drug substances, agrochemicals, and substances used for medical diagnostics.[1−3] The predominant structures are aryl fluorides and trifluoromethylated arenes.[4,5] In contrast, alkyl fluoride motifs are far less abundant in small molecules relevant for life sciences. Nevertheless, recent studies have highlighted the beneficial properties of alkyl fluorides for the modification of molecular conformation, polarity, acid−base properties, and electronic interactions based on *gauche*/anomeric effects.[6−14] There are a few examples of marketed alkyl fluoride drugs, such as macrolide antibiotics solithromycin, fluticasone, and sofosbuvir, which are used for treatment of asthma and hepatitis C (Figure 1a).[4] One of the main reasons for the relatively low abundance of fluoroalkyl motifs in pharmaceutical compounds is attributed to methodological limitations for the selective synthesis of alkyl fluorides, especially with tertiary C−F stereocenters (Figure 1a).[15] On the basis of our previous results on fluorocyclization of alkenes with fluorobenziodoxol (a hypervalent iodine reagent),[16] we decided to develop an asymmetric version of this reaction to access heterocyclic compounds with endocyclic tertiary fluoride motifs.

Chiral hypervalent iodines have become attractive catalysts and mediators for asymmetric oxidation reactions.[17−20] These species have been successfully employed for a wide range of enantioselective C−C,[21−23] C−O,[24−28] and C−N[29,30] bond formation reactions using alkene derivatives as substrates. The groups of Kitamura,[31] Jacobsen,[32] and Gilmour[33] reported pioneering methods for catalytic fluorination of olefins with *in situ* generated iodine(III) fluorides. Chiral iodine(III) fluorides were first applied by Nevado and co-workers for the asymmetric synthesis of fluorinated compounds, such as piperidines and azepanes.[34] This seminal work has been followed by several catalytic asymmetric protocols.[35−40]

As mentioned above, enantioselective construction of tertiary fluorides is considered to be particularly challenging but relevant for drug design (Figure 1a) and for modern synthetic methodology development.[15] Although many excellent techniques were reported for the synthesis of these species,[41−51] relatively few methods are based on hypervalent iodine reagents.[32,37,38,52−54] Jacobsen and co-workers presented studies on asymmetric aziridination[38] and 1,2-difluorination reactions[32,37] (Figure 1b) leading to tertiary fluorides. The groups of Rueping[52] and Lu/Zheng[53] described a method for the synthesis of chiral tertiary fluoro β-ketoesters using hypervalent iodine based catalysts. Fluorocyclization with hypervalent iodides[16,55−59] is a challenging but very efficient approach for accessing pharmaceutically important heterocycles, such as tetrahydrofurans and pyrrolidines. However, fluorocyclization for the synthesis of endocyclic chiral tertiary fluorides with hypervalent iodides (Figure 1c) has not been reported so far. In addition, the mechanistic features governing

Received: August 30, 2020
Published: November 16, 2020

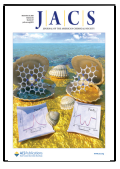

https://dx.doi.org/10.1021/jacs.0c09323
J. Am. Chem. Soc. 2020, 142, 20048−20057

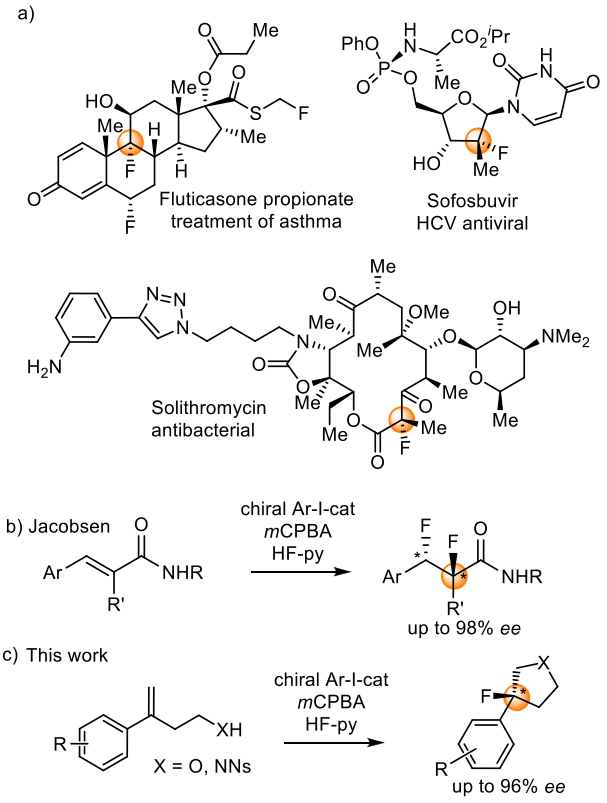

Figure 1. (a) Examples of drugs featuring tertiary fluoride centers. (b) Asymmetric construction of tertiary C−F stereocenters by difluorination. (c) Oxy- and aminofluorocyclization.

the reactivity and selectivity in these types of fluorocyclization reactions have been unexplored.

RESULTS AND DISCUSSION

In the initial fluorocyclization reactions we employed 1,1-disubstituted styrenes with tethered hydroxy groups as substrates in the presence of C_2-symmetric aryl iodide catalysts (Figure 2) with HF-pyridine as fluorine source and *m*CPBA as oxidant (Table 1). According to previous reports, catalysts

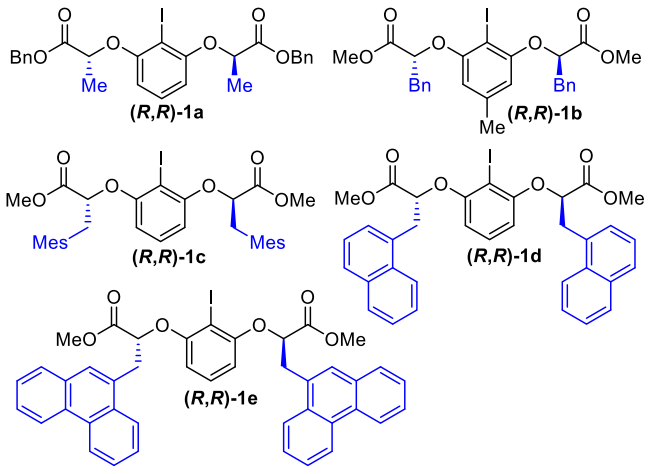

Figure 2. C_2-symmetric aryl iodine catalysts (*R,R*)-**1a−e** and new catalysts (*R,R*)-**1d,e** developed in this study. The so-called "side-arms" are given in blue color.

(*R,R*)-**1a−c** are particularly suitable for asymmetric fluorination reactions of alkenes (Figure 2).[34,38,56,60]

Table 1. Optimization of Reaction Conditions for the Asymmetric Oxyfluorination Reaction[a]

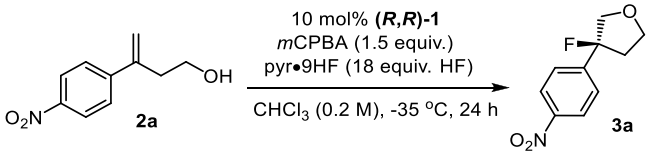

entry	catalyst	conditions[a]	ee[b] (%)	yield[c] (%)
1	(*R,R*)-**1a**	as indicated	72	41
2	(*R,R*)-**1b**	as indicated	88	50
3	(*R,R*)-**1c**	as indicated	90	75
4	(*R,R*)-**1d**	as indicated	93	83
5	(*R,R*)-**1e**	as indicated	88	66
6	(*R,R*)-**1c**	CH_2Cl_2 as solvent	74	63
7	(*R,R*)-**1c**	toluene as solvent	61	70
8	(*R,R*)-**1c**	0 °C	70	75
9	(*R,R*)-**1c**	0.1 M in $CHCl_3$	89	75
10	(*R,R*)-**1c**	9 equiv of HF	85	78
11	(*R,R*)-**1c**	5 mol % cat.	73	83
12	no cat.	as indicated		0

[a]Conditions: **2a** (0.1 mmol), (*R,R*)-**1** (0.01 mmol), pyr·9HF (0.2 mmol, pyr = pyridine), and *m*CPBA (0.15 mmol) dissolved in $CHCl_3$ (0.5 mL) at −35 °C and stirred for 24 h. [b]Enantiomeric excess determined by chiral SFC. [c]Isolated yield.

Optimization of the Reaction Conditions. We selected *p*-nitrostyryl alcohol **2a** as a model compound for the optimization of the reaction conditions. When the reaction was carried out under the conditions given in Table 1, using lactate-derived catalyst (*R,R*)-**1a**,[38] fluorotetrahydrofuran derivative **3a** was obtained with encouraging levels of ee (72%) and yield (41%) (Table 1, entry 1). The absolute configuration of the tertiary carbon−fluorine stereocenter in **3a** is (*S*) based on X-ray diffraction studies. When (*R,R*)-**1a** was replaced by phenyllactate catalyst (*R,R*)-**1b**,[38] both the yield (50%) and the enantioselectivity (88%) increased, probably because of the increased steric demand of the α-substituent in the so-called "side arm" of the ester group (entry 2). Possibilities to improve the stereoselectivity were further studied by increasing the size of the side arm substituent. Indeed, the use of mesityl lactate derivative (*R,R*)-**1c**[60] increased the enantioselectivity to 90% (entry 3).

This selectivity enhancement prompted us to study the subtle steric effect of the *ortho* substitution of the side arms. Therefore, we prepared two new catalysts, with naphthyl (*R,R*)-**1d** and phenanthryl (*R,R*)-**1e** groups in the side arms. To our delight, by use of the newly developed 1-naphthyllactate catalyst (*R,R*)-**1d**, the ee could be increased to 93%, affording **3a** with a high yield of 83% (entry 4). The naphthyl substituents of (*R,R*)-**1d** probably exert the ideal substituent effects in the stereoinduction step, as the ee of the reaction declined to 88% (entry 5) with the bulkier phenanthryllactate catalyst (*R,R*)-**1e**. An in-depth analysis on the substituent effects of the side-arms on the stereoinduction is given in the DFT/stereoinduction section below.

We briefly studied the solvent effects on the reaction. By use of catalyst (*R,R*)-**1c**, chloroform was replaced by methylene chloride and toluene. In both cases the enantioselectivities

https://dx.doi.org/10.1021/jacs.0c09323
J. Am. Chem. Soc. 2020, 142, 20048−20057

Scheme 1. Scope of the Oxyfluorination Reaction[a]

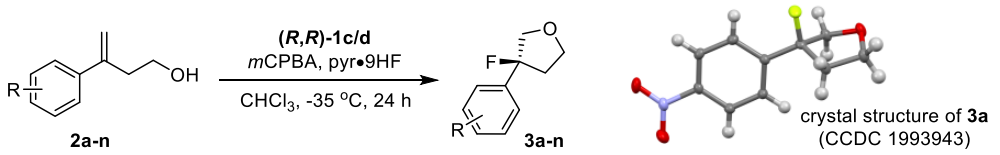

***p*-substitution**	**3a**	**3b**	**3c**	**3d**	**3e**	**3f**	**3g**	**3h**
(*R*,*R*)-1c	75%, 90% *ee* 84%, 89% *ee*[b]	49%, 90% *ee*	79%, 89% *ee*	49%, 73% *ee*	49%, 84% *ee*	63%, 85% *ee*	41%, 91% *ee*	60%, 91% *ee*
(*R*,*R*)-1d	83%, 93% *ee* 85%, 90% *ee*[c] 64%, 94% *ee*[d]	54%, 92% *ee*	68%, 92% *ee* 54%, 96% *ee*[d]	52%, 88% *ee*	58%, 86% *ee* 34%, 94% *ee*[d]	79%, 87% *ee*	27%, 92% *ee*	63%, 89% *ee*

***m*-substitution**	**3i**	**3j**	**3k**	***o*-substitution**	**3l**	**3m**	**3n**
(*R*,*R*)-1c	83%, 82% *ee*	44%, 79% *ee*	41%, 59% *ee*		40%, -33% *ee*	42%, 16% *ee*	n.o., -
(*R*,*R*)-1d	88%, 86% *ee* 61%, 95% *ee*[d]	37%, 82% *ee*	36%, 61% *ee*		41%, +39% *ee*	35%, 30% *ee*	

[a]Conditions: **2a** (0.1 mmol), (***R*,*R***)-**1** (0.01 mmol), pyr·9HF (0.2 mmol), and *m*CPBA (0.15 mmol) dissolved in $CHCl_3$ (0.5 mL) at −35 °C and stirred for 24 h. Enantiomeric excess determined by chiral SFC. Isolated yield. [b]0.5 mmol scale reaction with catalyst (***R*,*R***)-**1c**. [c]1 mmol scale reaction with catalyst (***R*,*R***)-**1d**. [d]The reaction was conducted at −50 °C for 60 h.

decreased (cf. entry 2 with entries 6 and 7). Conducting the reaction at 0 °C did not influence the yield, but the enantioselectivity was lower (entry 8). Dilution (entry 9) and decrease of the amount of HF-pyridine (entry 10) led to a slight decrease of the ee and the same or improved yield. Decreasing of the amount of catalyst from 10% to 5% (entry 11) decreased the ee to 73%. The decrease of the ee was surprising as in the absence of catalyst formation of **3a** was not observed (entry 12). This indicates that there is no racemic background reaction in the absence of iodoaryl catalyst. We found (see Supporting Information for experimental studies, page S65) that the catalyst did not undergo racemization under the applied reaction conditions. This control experiment (Supporting Information, page S65) suggests that the catalyst underwent transformation/degradation under the applied oxidative conditions and perhaps these products also catalyzed the fluorocyclization, albeit with lower selectivity than (***R*,*R***)-**1c,d**. Unfortunately, we were unable to isolate these degradation products of the catalyst. In a very recent publication, Sigman, Jacobsen, and co-workers[54] reported the isolation of chiral iodoresorcinol derivatives, which were formed under the oxidative conditions and still catalyzed the difluorination reactions.

Tetrahydrofurans by Asymmetric Fluorocyclization. Since both catalysts (***R*,*R***)-**1c** and (***R*,*R***)-**1d** induced high levels of enantioselectivities and good yields, we decided to explore the substrate scope of the reaction with both catalysts (Scheme 1). We studied the effects of the aromatic substituents on the reactivity of the styrene substrates and on the enantioselectivity of the fluorocyclization (Scheme 1).

Para-substituted styrenes (**2a**−**h**) reacted with somewhat higher selectivity (typically around 90% ee) than the *meta*-substituted ones (**2i**−**k**). The fluorocyclization of *ortho*-substituted styrenes (**2l**,**m**) proceeded with low selectivity and decreased reactivity. Both catalysts induced high enantioselectivity, but the ee values were higher with the newly developed 1-naphthyllactate catalyst (***R*,*R***)-**1d**, than with the mesityl analog (***R*,*R***)-**1c**. Nitro-, trifluoromethyl-, and methyl sulfone-substituted fluorotetrahydrofurans **3a**−**c** formed with high ee (92−93%) and good yield (54−83%) using naphthyllactate catalyst (***R*,*R***)-**1d**.

Somewhat lower enantioselectivities (73−88% ee) were observed for the formation of nitrile-, keto-, and ester-substituted products **3d**−**f**. Interestingly, benzamide **3g** and tertiary benzamide **3h** were formed with high levels of enantioselectivity (up to 92% ee). However, the yield of the primary amide **3g** was only 27%/41% (with (***R*,*R***)-**1d**/(***R*,*R***)-**1c**) probably because of poor solubility of the corresponding substrate (**2g**) in chloroform. As mentioned above, *meta*-substituted products **3i**−**k** were formed with lower selectivity. While *para*-nitro derivative **3a** was formed with 93% ee, its *meta*-nitro analog **3i** was obtained with 86% ee using catalyst (***R*,*R***)-**1d**. Similarly, *meta*-methylcarbonyl compound **3j** was obtained with 82% ee, while the *para*-substituted isomer **3e** was formed with 86% ee. In the case of *meta*-benzyl ether substitution (**3k**) the fluorocyclization proceeded with relatively low ee (61%) and poor yield (36%). Fluorocyclization of *ortho*-cyano-substituted styrene **2l** with catalyst (***R*,*R***)-**1d** resulted in formation of **3l** with 39% ee. Surprisingly, the reaction with catalyst (***R*,*R***)-**1c** gave the opposite enantiomer *ent*-**3l** with 33% ee. In the case of an *ortho*-chloro substituent, the major enantiomer formed with the same configuration using either (***R*,*R***)-**1c** or (***R*,*R***)-**1d**, albeit with low ee of 16% or 30%, respectively. While *para*- and *meta*-substituted nitro aryl

https://dx.doi.org/10.1021/jacs.0c09323
J. Am. Chem. Soc. 2020, 142, 20048−20057

Scheme 2. Control Experiments

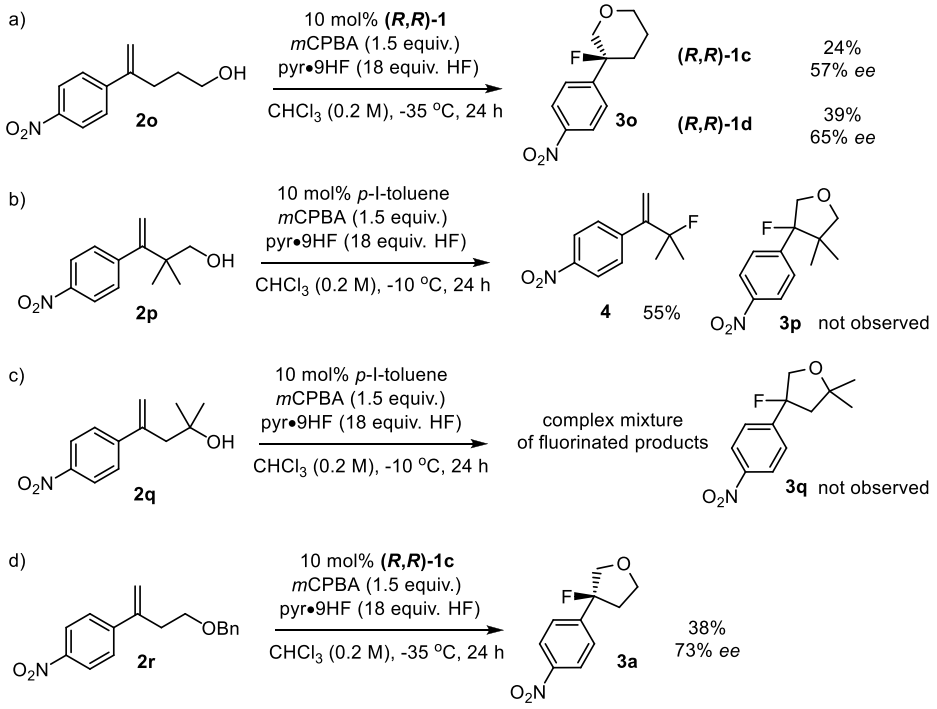

derivatives **3a** and **3i** formed with high ee's and yields, formation of the *ortho*-substituted analog **3n** was not observed. The effects of the *ortho*-nitro substitution on fluorination and fluorocyclization reactions have been previously reported.[39,60] As shown in Table 1, the reaction of **2a** gave a higher enantioselectivity at a lower temperature (cf. Table 1, entries 3 and 8). Therefore, we carried out the reaction of some substrates at −50 °C using (***R,R***)**-1d** as catalyst, to see whether the enantioselectivity could be further increased. We found that the *para*-substituted substrates **2a**, **2c**, **2e** and *meta*-substituted substrate **2i** reacted with higher enantioselectivities (94−96%) at −50 °C than at −35 °C (86−93%). However, the yields were lower at −50 °C than at −35 °C. The lower yields at −50 °C have been a consequence of the lower reactivity, which may be caused by solubility issues. The reactions can be easily scaled up without significant change of the selectivity or yield. For example, under the standard optimized conditions **3a** was obtained with 89% ee (0.5 mmol scale) and 90% ee (1 mmol scale) using catalysts (***R,R***)**-1c** and (***R,R***)**-1d**, respectively.

We have also studied the effects of the alteration of the aliphatic tether of the alcohol nucleophile (Scheme 2a−c). When the carbon chain was elongated by a single methylene unit, the corresponding tetrahydropyran **3o** was formed in lower yield (24%/39%) and selectivity (57%/65% ee) than **3a** using (***R,R***)**-1c** or (***R,R***)**-1d** as catalyst (Scheme 2a). We did not observe formation of tetrahydrofuran products. The lack of five membered ring (tetrahydrofuran) products indicates that the elongation of the tether did not lead to change of the mechanism of the fluorocyclization involving a phenonium ion intermediate.[36,57,59,61−63] Possible reasons to explain the drop of the ee on elongation of the tether are given below in the DFT/stereoinduction section. We have also attempted to study the Thorpe−Ingold effect[64,65] on the reactivity of the substrates by dimethyl substitution of the tether (Scheme 2b,c). However, formation of fluorocyclization products **3p,q** was not observed using *para*-iodotoluene as catalyst. In the case of the attempted fluorocyclization of **2p**, allyl fluoride **4** formed (Scheme 2b). The mechanism of this reaction involving a formal extrusion of a CH_2O molecule is unclear. When fluorocyclization of **2q** was attempted, a complex reaction mixture of various fluorinated products was obtained (Scheme 2c). In addition, we also studied the effects of protection of the alcohol nucleophile (Scheme 2d). In the reaction of benzyl protected substrate **2r**, the same fluorocyclization product **3a** was observed as with the parent alcohol (**2a**), albeit with lower yield (38%) and selectivity (73% ee). Formation of the identical major enantiomer with **2a** and **2r** under the same reaction conditions indicates that the enantioselectivity is not controlled by the nucleophilicity of the oxygen, which means that the cyclization process is not involved in the enantiodetermining step of the oxyfluorination. This suggests that the enantioselectivity is determined in the fluorination process.[60,62]

Extension to Pyrrolidines. The asymmetric fluorocyclization reaction of alcohol nucleophiles **2** can be extended to sulfonate-protected nitrogen nucleophiles **5** (Table 2). We have found that the selectivity of the aminofluorination reaction is dependent on the sulfonyl protecting group. The fluorocyclization of sulfonamide analogs (**6a−c**) of nitro compound **3a** was studied (Table 2) under the optimal conditions of the oxyfluorination (Table 1, entry 4). Formation of pyrrolidine derivatives **6a** and **6c** (70%/72% ee) with nosyl and mesyl protecting groups (Table 2, entries 1 and 3) occurred with higher selectivity than with tosyl-substituted (entry 2) analog **6b** (56% ee). Similar to the results obtained for oxyfluorination reactions, application of our newly developed 1-naphthyllactate catalyst (***R,R***)**-1d** gave higher selectivity than the mesityl derivative (***R,R***)**-1c** (cf. entries 1 and 4). A slight change of the applied amount of pyr•9HF reagent and dilution of the reaction mixture led to an increase of the ee from 70% to 75% (cf. entries 1 and 5). The difference

https://dx.doi.org/10.1021/jacs.0c09323
J. Am. Chem. Soc. 2020, 142, 20048−20057

Table 2. Screening of N-Protection for the Asymmetric Aminofluorination Reaction[a]

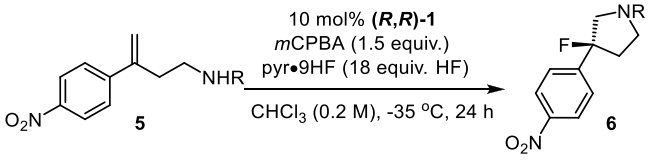

entry	catalyst		ee[b] (%)	yield[c] (%)
1	(*R,R*)-**1d**	**6a** R = Ns	70	58
2	(*R,R*)-**1d**	**6b** R = Ts	56	68
3	(*R,R*)-**1d**	**6c** R = Ms	72	63
4	(*R,R*)-**1c**	**6a**	62	59
5[d]	(*R,R*)-**1d**	**6a**	75	76

[a]Conditions: Unless otherwise stated **5** (0.1 mmol), (*R,R*)-**1** (0.01 mmol), pyr·9HF (0.2 mmol), and *m*CPBA (0.15 mmol) dissolved in $CHCl_3$ (0.5 mL) at −35 °C and stirred for 24 h. [b]Enantiomeric excess determined by chiral SFC. [c]Isolated yield. [d]Using pyr·9HF (0.3 mmol) in $CHCl_3$ (1.0 mL).

in selectivity for the nosyl- (**6a**) and mesyl-substituted (**6c**) products was relatively small. As the nosyl protection group is easier to remove than the mesyl group, we selected nosyl protection for the study of the synthetic scope of the reaction.

By use of the optimal conditions (Table 2, entry 5), pyrrolidine derivatives with tertiary C−F bonds were obtained (Scheme 3) with high selectivity (up to 94% ee, **6e**). The enantioselectivity of the aminocyclization reactions (Scheme 3) was slightly lower, but the yields were somewhat higher than for the oxyfluorination reactions (Scheme 2). Pyrrolidine derivatives with trifluoromethyl- (**6d**), cyano- (**6f**), and methyl ester- (**6h**) substitution formed with the highest selectivity (86−92% ee). Nitro- (**6a**), methyl sulfonyl- (**6e**), methyl carbonyl- (**6g**), and dimethylamide (**6i**) products were obtained with lower enantioselectivity (72−82% ee) than the corresponding tetrahydrofuran analogs (86−93% ee). The absolute configuration of **6e** is (*S*) according to the X-ray crystallography data. The fact that the absolute configuration of tetrahydrofuran **3a** and pyrrolidine **6e** formed under similar reaction conditions with the same (*S*) absolute configuration and with similar levels of enantioselectivities indicates that the mechanism and stereoinduction in the asymmetric oxyfluorination and aminofluorination reactions are closely similar.

Similar to the oxyfluorination processes, the aminofluorination reactions of *meta*-substituted substrates (**5j,k**) proceeded with similar or lower selectivity (75%/68% ee) than the *para*-substituted analogs (75%/82% ee for **6a**/**6g**). Alkyl-substituted alkene derivative **5l** also underwent fluorocyclization reaction affording **6l** in 56% yield. However, the enantioselectivity (39% ee) was much lower than for the aromatic analogs indicating the important role of the aromatic substituent in the stereoselection process. As expected, some of the aminofluorination reactions proceeded with higher selectivity at −50 °C than at −35 °C. Using (*R,R*)-**1d** as catalyst, we also carried out the fluorocyclization reactions of *para*-substituted compounds **5a**, **5e**, **5g** and *meta*-substituted compounds **5j** and **5k** at −50 °C. The enantioselectivity increased in all reactions, but the yield decreased. A substantial improvement of the selectivity was observed for the formation of sulfone-substituted fluoropyrrolidine **6e**, which was obtained with excellent ee (94%) and in good yield (56%) at −50 °C. Similar to the oxyfluorination reactions, several other substrates reacted with very low yield at −50 °C. The nosyl group can

Scheme 3. Scope of Aminofluorination Reaction[a]

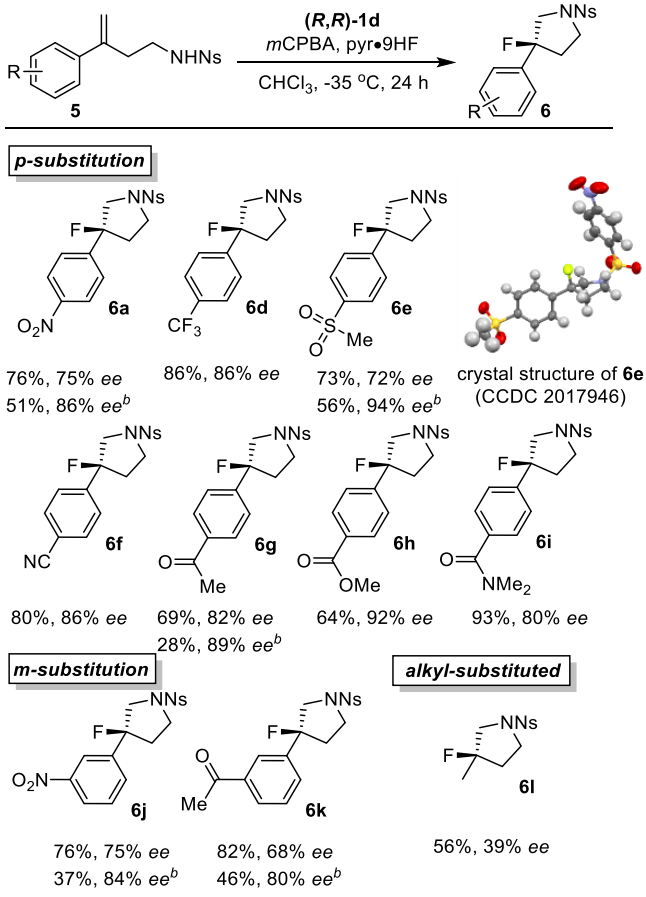

[a]Conditions: **5** (0.1 mmol), (*R,R*)-**1d** (0.01 mmol), pyr·9HF (0.3 mmol), and *m*CPBA (0.15 mmol) dissolved in $CHCl_3$ (1.0 mL) at −35 °C and stirred for 24 h. Enantiomeric excess determined by chiral SFC. Isolated yield. [b]The reaction was conducted at −50 °C for 60 h.

be easily removed from the pyrrolidine ring without affecting the enantiopurity of the products (Scheme 4). For example,

Scheme 4. Deprotection of Product 6d

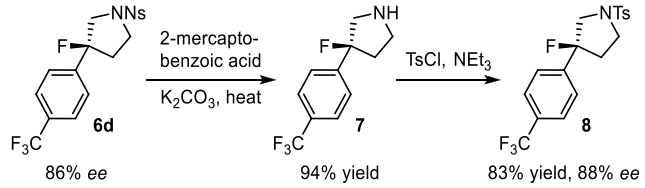

treatment of **6d** with 2-mercaptobenzoic acid in the presence of K_2CO_3 leads to the free amine product **7**. We were not able to determine the enantiopurity of **7**, and therefore it was protected with a tosyl group (**8**). The ee of the tosylated product **8** indicated that the deprotection of the nosyl derivative **6d** did not lead to decrease of the enantiopurity.

DFT Modeling Studies. In order to gain mechanistic insights into the fluorocyclization reactions, we performed density functional theory (DFT) calculations, using nitrophenyl styrene **2a** as a model substrate, with (*R,R*)-**1c** as catalyst (Table 1, entry 3). The calculations were carried out using the B3LYP-D3 functional,[66−69] and implicit solvation using the SMD[70] model with the parameters for chloroform

https://dx.doi.org/10.1021/jacs.0c09323
J. Am. Chem. Soc. 2020, 142, 20048−20057

was included in the geometry optimizations (see Supporting Information for computational details).

Catalytic Cycle and Reaction Profile. The reaction mechanism for the fluorocyclization of **2a** obtained from the calculations is shown in Scheme 5. The associated free energy profile is displayed in Figure 3, and the optimized geometries of the intermediates and transition states are given in the Supporting Information for the computational part. The catalytic cycle starts with the formation of (R,R)-**1c-F$_2$** by oxidation and deoxyfluorination of iodoarene (R,R)-**1c**. This step was not considered explicitly by the calculations, but the formation of (R,R)-**1c-F$_2$** is supported by experiments that confirm the oxidation of iodoarene by *m*CPBA to form the iodosylarene (ArI=O), which is readily converted to the difluorinated species by reaction with HF.[35,71−73]

Scheme 5. Catalytic Cycle Based on DFT Calculations for Fluorocyclization of 2a with Hypervalent Iodine Catalyst (R,R)-1c

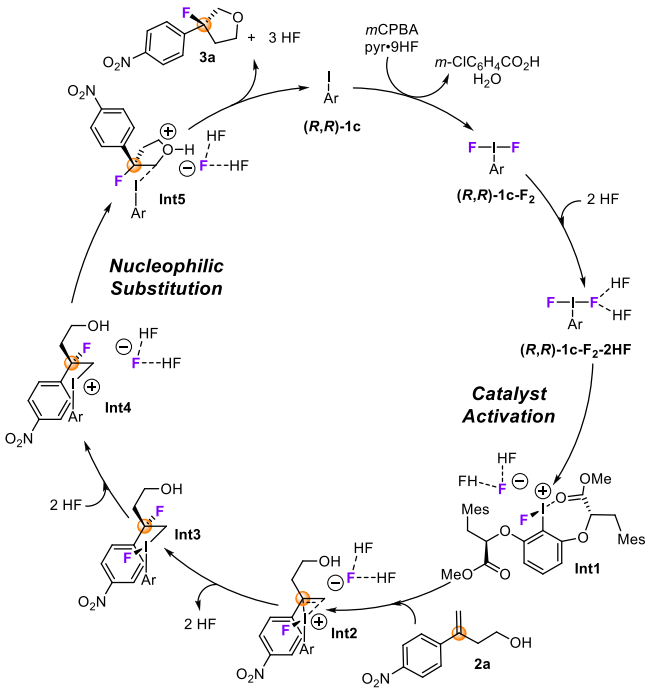

The next step of the cycle is the loss of a fluoride from (R,R)-**1c-F$_2$** to yield the cationic fluoroiodonium active catalytic species **Int1**. Similar to the mechanism proposed by Jacobsen, Xue, and Houk for the aryl iodine-catalyzed asymmetric difluorination of β-substituted styrenes,[62] we employed two molecules of HF as an activation model for the iodoarene difluoride. Coordination of the two HF molecules results in the formation of the hydrogen-bonded difluoride complex (R,R)-**1c-F$_2$-2HF**, which is 0.6 kcal/mol lower than (R,R)-**1c-F$_2$**. Then, abstraction of fluoride occurs through transition state **TS1**, which is 18.7 kcal/mol higher than (R,R)-**1c-F$_2$-2HF**, resulting in intermediate **Int1**.

In line with the results on the aryl iodine-catalyzed asymmetric difluorination of β-substituted styrenes,[62] the transformation of (R,R)-**1c-F$_2$** to **Int1** is assisted by one of the carbonyl groups of the side chain of the catalyst through an $I^+\cdots O$ interaction that also stabilizes the cationic species **Int1**. Note that **Int1** here is modeled as an ion-pair, consisting of a cationic catalyst species and an $(HF)_2F^-$ counterion. Many (>20) initial geometries of this ion-pair complex were considered in order to make sure that the lowest-energy conformation is located (the same applies to **Int2**, **Int4**, **TS3**, and **Int5** below). We have also calculated the case in which the ions (i.e., $(HF)_2F^-$ and the cationic part) are separated. The two different approaches led to some significant changes in the energy profiles but not to the mechanistic conclusions (see comparison in the Supporting Information for computational details on page S3).

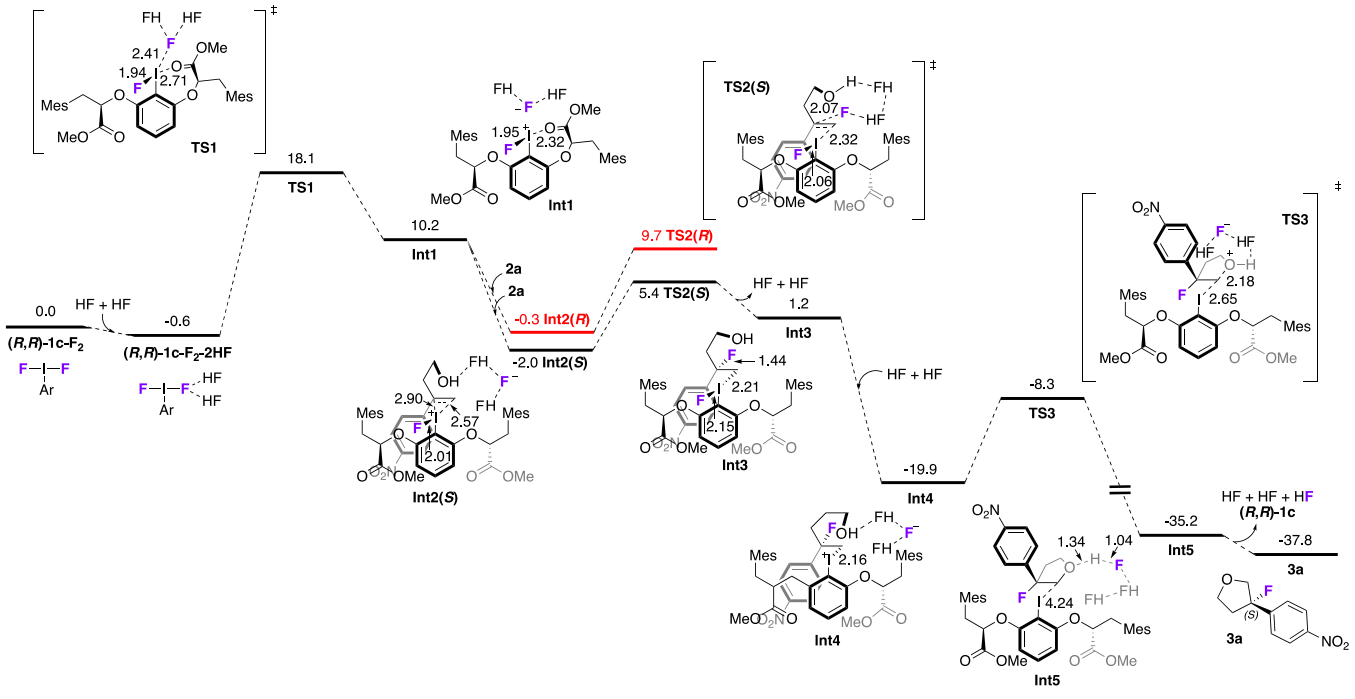

Figure 3. Calculated free energy profile (kcal/mol) for the aryl iodine-catalyzed oxyfluorination of **2a** with (R,R)-**1c**.

https://dx.doi.org/10.1021/jacs.0c09323
J. Am. Chem. Soc. 2020, 142, 20048−20057

In the next step, substrate **2a** coordinates to **Int1** to give iodonium ion intermediate **Int2(*S*)**, which is calculated to be 12.2 kcal/mol lower in energy than **Int1**. The coordination can take place with either the *Si* or *Re* face of the double bond. In this case it was found that the coordination to *Re*-face was lower in energy, which will have implications on the enantioselectivity of the reaction (see "stereoinduction" section below). We made many attempts to locate the transition state for the coordination of the olefin but without success. The optimizations led always to **Int2(*S*)**.

The olefin then undergoes a nucleophilic attack by the $(HF)_2F^-$ counterion at the most substituted carbon (via **TS2(*S*)**), generating **Int3**, in which two new σ-bonds are formed (C–I at 2.21 Å and C–F at 1.44 Å) and the double bond of the substrate is converted into a single bond. The barrier for this step is calculated to be 7.4 kcal/mol relative to **Int2(*S*)**. We also considered the possibility of intramolecular attack by the hydroxyl group at the iodine(III)-activated alkene (see Supporting Information for computational details, S5). However, this mechanistic scenario was found to be associated with a considerably higher barrier than **TS2(*S*)**. These results are also in line with our control experiment (Scheme 2d) indicating that the enantioselectivity is determined in the fluorination process prior to the cyclization step. The formation of the C–I bond in **Int3** weakens the I–F bond (2.15 Å in **Int3** vs 2.01 Å in **Int2(*S*)**), which makes the dissociation of fluoride easier. According to the calculations, two HF molecules can abstract the fluoride to yield ion-pair intermediate **Int4**, which is 21.1 kcal/mol lower than the neutral iodoarene intermediate **Int3**. Next, an intramolecular nucleophilic attack by the oxygen atom of **2a** displaces the aryliodonium moiety, which is an excellent leaving group. The step occurs via **TS3**, with a barrier of 11.6 kcal/mol, and the resulting **Int5** that contains the protonated form of the cyclic product **3a** is 15.3 kcal/mol lower than **Int4** (Figure 3). The last step of the cycle is the deprotonation of the protonated cyclic compound to give the final product **3a** and regenerate the iodoarene catalyst (***R*,*R*)-1c**. The $(HF)_2F^-$ counterion can achieve this step, which is calculated to be exergonic by 2.6 kcal/mol.

Factors Determining the Stereoselection. The overall energy profile obtained for the mechanism (Figure 3) shows that the coordination of substrate **2a** to **Int1** to form **Int2(*S*)** is an irreversible process. The coordination of the substrate can take place with either the *Re* or *Si* faces of the double bond, resulting in **Int2(*S*)** or **Int2(*R*)**, respectively, indicating that this is the selectivity-determining step of the reaction. **Int2(*S*)** leads ultimately to the *S*-enantiomer (major enantiomer according to the experimental studies) of the product, while **Int2(*R*)** leads to the *R*-enantiomer. As mentioned above, it was not possible to locate the transition state for this coordination step. Instead, we optimized the geometry of **Int2(*R*)**, which was found to be 1.7 kcal/mol higher in energy than **Int2(*S*)**. Subsequently, the potential energy surface was calculated backward from these intermediates. Thus, we performed constrained optimizations starting from **Int2(*S*)** and **Int2(*R*)**, in which the distance between the iodine center and the double bond of the substrate was increased gradually (see S6 in the Supporting Information for computational studies). This procedure shows that the energy difference between the intermediates is maintained along the reaction coordinate of the coordination, even at long distances that resemble the TS structures. The calculated energy difference is in good agreement with the experimentally observed ee of 90% in favor of the *S*-product (Table 1, entry 3), indicating that the factors governing the enantioselectivity can be deduced by analyzing the geometries of **Int2(*S*)** and **Int2(*R*)**, as shown in Figure 4. Scrutiny of these geometries shows that the substrate

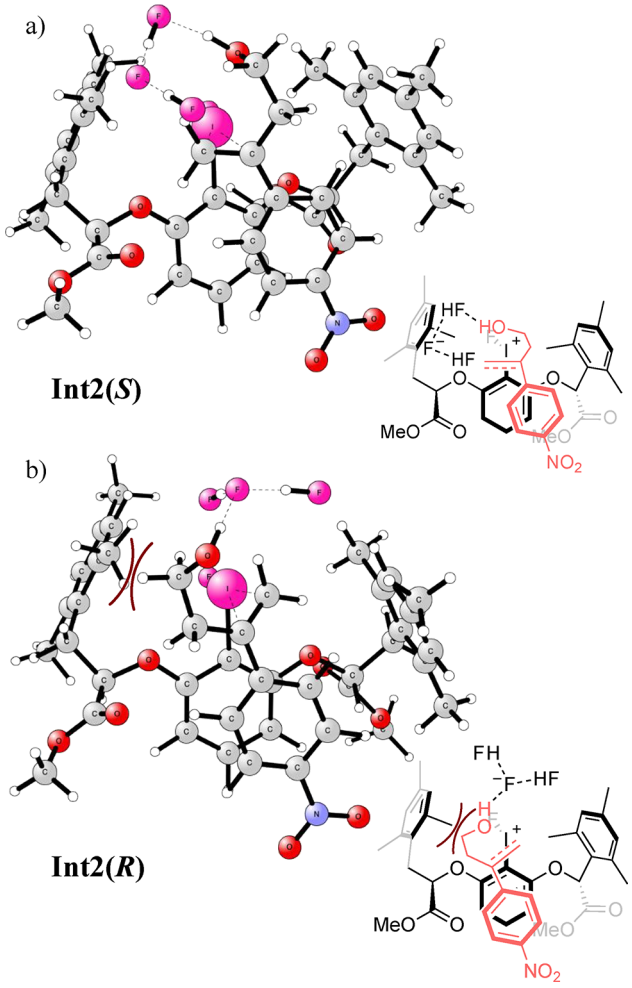

Figure 4. Optimized geometries of the intermediates resulting from the coordination of substrate **2a** to **Int1**. (a) **Int2(*S*)**: coordination from the *Re*-face, leading to the *S*-product. (b) **Int2(*R*)**: coordination from the *Si*-face, leading to the *R*-product.

in **Int2(*S*)** fits better into the chiral pocket of the catalyst as compared to the **Int2(*R*)** (Figure 4). Namely, **Int2(*R*)** is destabilized by a steric repulsion between one of the *ortho*-methyl substituents of the aryl group of the catalyst side arms and one of the methylene carbons of substrate **2a** (Figure 4b).

The *ortho*-substituents in the side arm of the catalyst thus play an important role in the stereoinduction, explaining why the enantioselectivity is affected by the variation of these substituents in the experiments (Figure 2 and Table 1). On the basis of this stereoselection model, we also conclude that elongation of the tether, such as in **2o**, leads to more repulsive interactions in both homologs of **Int2(*S*)** and **Int2(*R*)**, leading to lower selectivity in fluorocyclization of **2o** (57% ee) than for **2a** (90% ee). In addition, this stereochemical model suggests that the presence of *ortho*-substituents in the substrates (such as in **3l–n**) generates major clashes with the iodoresorcinol catalysts in the intermediates corresponding to **Int2(*S*)** and

https://dx.doi.org/10.1021/jacs.0c09323
J. Am. Chem. Soc. 2020, 142, 20048–20057

Int2(*R*), which leads to a major drop (**3m**) or even inversion (**3l**) of the stereoselectivity.

CONCLUSIONS

In summary, we have developed a new method for the synthesis of chiral tetrahydrofurans and pyrrolidines with endocyclic tertiary C−F stereocenters. The fluorocyclization reactions of various 1,1-disubstituted styrene derivatives were catalyzed by *in situ* generated hypervalent iodines. The best selectivities (up to 96% ee) were achieved using a newly developed catalyst, (*R*,*R*)-**1d**, with 1-naphthyl substituents in the side arm. Our experimental findings suggest that the selectivity of the reaction is dependent on the effects of substituents attached to the aromatic ring in the styrene substrates. DFT modeling was conducted to rationalize the factors governing the enantioselectivity in the fluorocyclization reaction resulting the tetrahydrofuran product. We present a new stereoselection model for formation of a tertiary C*−F bond using hypervalent iodine catalyst in an internal oxyfluorination reaction. The calculations show that the major factor determining the selectivity is a steric repulsion between the side arm substituent of the chiral catalyst and one of the methylene groups in the tether of the oxygen nucleophile. Our stereoselection model also accounts for the drop of the stereoselectivity on elongation of the tether of the nucleophile, as well as the adverse effects of *ortho* substituents in the aromatic ring of the styrene substrates. The above study forwards the catalytic asymmetric syntheses of tertiary fluorides, which are considered to be one of the most challenging methodological problems in organic synthesis.[15] Extension of the toolbox of asymmetric catalysis to access tertiary fluorides is important to increase the molecular diversity of complex organofluorine species used in life-sciences, such as in drug development (Figure 1a).[4,15]

ASSOCIATED CONTENT

Supporting Information

The Supporting Information is available free of charge at https://pubs.acs.org/doi/10.1021/jacs.0c09323.

Experimental procedures, characterization data, and NMR spectra of compounds (PDF)

Computational details and additional computational results discussed in the text, absolute energies and energy corrections, and Cartesian coordinates (PDF)

X-ray crystal structure file for compound **3a** (CIF)

X-ray crystal structure file for compound **6e** (CIF)

AUTHOR INFORMATION

Corresponding Authors

Fahmi Himo − *Department of Organic Chemistry, Stockholm University, SE-106 91 Stockholm, Sweden;* orcid.org/0000-0002-1012-5611; Email: fahmi.himo@su.se

Kálmán J. Szabó − *Department of Organic Chemistry, Stockholm University, SE-106 91 Stockholm, Sweden;* orcid.org/0000-0002-9349-7137; Email: kalman.j.szabo@su.se

Authors

Qiang Wang − *Department of Organic Chemistry, Stockholm University, SE-106 91 Stockholm, Sweden;* orcid.org/0000-0003-4346-8714

Marvin Lübcke − *Department of Organic Chemistry, Stockholm University, SE-106 91 Stockholm, Sweden;* orcid.org/0000-0002-7276-2755

Maria Biosca − *Department of Organic Chemistry, Stockholm University, SE-106 91 Stockholm, Sweden;* orcid.org/0000-0002-9116-6318

Martin Hedberg − *Department of Organic Chemistry, Stockholm University, SE-106 91 Stockholm, Sweden*

Lars Eriksson − *Department of Materials and Environmental Chemistry, Stockholm University, SE-106 91 Stockholm, Sweden*

Complete contact information is available at: https://pubs.acs.org/10.1021/jacs.0c09323

Author Contributions

[§]Q.W., M.L., and M.B. contributed equally.

Notes

The authors declare no competing financial interest.

ACKNOWLEDGMENTS

The authors thank the Knut och Alice Wallenbergs Foundation (Dnr 2018.0066) and Swedish Research Council (Dnr 2017-04235) for financial support. A postdoctoral fellowship for Q.W. is gratefully acknowledged to Stiftelsen Olle Engkvist Byggmästare (Dnr 192-0484). We thank Matteo Costantini for his kind help with chiral HPLC analyses.

REFERENCES

(1) Jeschke, P. The Unique Role of Fluorine in the Design of Active Ingredients for Modern Crop Protection. *ChemBioChem* **2004**, *5*, 570−589.

(2) Müller, K.; Faeh, C.; Diederich, F. Fluorine in Pharmaceuticals: Looking Beyond Intuition. *Science* **2007**, *317*, 1881−1886.

(3) Purser, S.; Moore, P. R.; Swallow, S.; Gouverneur, V. Fluorine in medicinal chemistry. *Chem. Soc. Rev.* **2008**, *37*, 320−330.

(4) Zhou, Y.; Wang, J.; Gu, Z.; Wang, S.; Zhu, W.; Aceña, J. L.; Soloshonok, V. A.; Izawa, K.; Liu, H. Next Generation of Fluorine-Containing Pharmaceuticals, Compounds Currently in Phase II−III Clinical Trials of Major Pharmaceutical Companies: New Structural Trends and Therapeutic Areas. *Chem. Rev.* **2016**, *116*, 422−518.

(5) Mei, H.; Han, J.; Fustero, S.; Medio-Simon, M.; Sedgwick, D. M.; Santi, C.; Ruzziconi, R.; Soloshonok, V. A. Fluorine-Containing Drugs Approved by the FDA in 2018. *Chem. - Eur. J.* **2019**, *25*, 11797−11819.

(6) Huchet, Q. A.; Kuhn, B.; Wagner, B.; Kratochwil, N. A.; Fischer, H.; Kansy, M.; Zimmerli, D.; Carreira, E. M.; Müller, K. Fluorination Patterning: A Study of Structural Motifs That Impact Physicochemical Properties of Relevance to Drug Discovery. *J. Med. Chem.* **2015**, *58*, 9041−9060.

(7) Linclau, B.; Wang, Z.; Compain, G.; Paumelle, V.; Fontenelle, C. Q.; Wells, N.; Weymouth-Wilson, A. Investigating the Influence of (Deoxy)fluorination on the Lipophilicity of Non-UV-Active Fluorinated Alkanols and Carbohydrates by a New log P Determination Method. *Angew. Chem., Int. Ed.* **2016**, *55*, 674−678.

(8) Jeffries, B.; Wang, Z.; Graton, J.; Holland, S. D.; Brind, T.; Greenwood, R. D. R.; Le Questel, J.-Y.; Scott, J. S.; Chiarparin, E.; Linclau, B. Reducing the Lipophilicity of Perfluoroalkyl Groups by CF2−F/CF2−Me or CF3/CH3 Exchange. *J. Med. Chem.* **2018**, *61*, 10602−10618.

(9) Graton, J.; Compain, G.; Besseau, F.; Bogdan, E.; Watts, J. M.; Mtashobya, L.; Wang, Z.; Weymouth-Wilson, A.; Galland, N.; Le Questel, J.-Y.; Linclau, B. Influence of Alcohol β-Fluorination on Hydrogen-Bond Acidity of Conformationally Flexible Substrates. *Chem. - Eur. J.* **2017**, *23*, 2811−2819.

(10) Thiehoff, C.; Rey, Y. P.; Gilmour, R. The Fluorine Gauche Effect: A Brief History. *Isr. J. Chem.* **2017**, *57*, 92−100.
(11) Aufiero, M.; Gilmour, R. Informing Molecular Design by Stereoelectronic Theory: The Fluorine Gauche Effect in Catalysis. *Acc. Chem. Res.* **2018**, *51*, 1701−1710.
(12) Bentler, P.; Bergander, K.; Daniliuc, C. G.; Mück-Lichtenfeld, C.; Jumde, R. P.; Hirsch, A. K. H.; Gilmour, R. Inverting Small Molecule−Protein Recognition by the Fluorine Gauche Effect: Selectivity Regulated by Multiple H→F Bioisosterism. *Angew. Chem., Int. Ed.* **2019**, *58*, 10990−10994.
(13) O'Hagan, D. Polar organofluorine substituents: Multivicinal fluorines on alkyl chains and alicyclic rings. *Chem. - Eur. J.* **2020**, *26*, 7981−7997.
(14) Nairoukh, Z.; Strieth-Kalthoff, F.; Bergander, K.; Glorius, F. Understanding the Conformational Behavior of Fluorinated Piperidines: The Origin of the Axial-F Preference. *Chem. - Eur. J.* **2020**, *26*, 6141−6146.
(15) Zhu, Y.; Han, J.; Wang, J.; Shibata, N.; Sodeoka, M.; Soloshonok, V. A.; Coelho, J. A. S.; Toste, F. D. Modern Approaches for Asymmetric Construction of Carbon−Fluorine Quaternary Stereogenic Centers: Synthetic Challenges and Pharmaceutical Needs. *Chem. Rev.* **2018**, *118*, 3887−3964.
(16) Yuan, W.; Szabó, K. J. Catalytic Intramolecular Aminofluorination, Oxyfluorination, and Carbofluorination with a Stable and Versatile Hypervalent Fluoroiodine Reagent. *Angew. Chem., Int. Ed.* **2015**, *54*, 8533−8537.
(17) Fujita, M. Mechanistic aspects of alkene oxidation using chiral hypervalent iodine reagents. *Tetrahedron Lett.* **2017**, *58*, 4409−4419.
(18) Claraz, A.; Masson, G. Asymmetric iodine catalysis-mediated enantioselective oxidative transformations. *Org. Biomol. Chem.* **2018**, *16*, 5386−5402.
(19) Flores, A.; Cots, E.; Bergès, J.; Muñiz, K. Enantioselective Iodine(I/III) Catalysis in Organic Synthesis. *Adv. Synth. Catal.* **2019**, *361*, 2−25.
(20) Parra, A. Chiral Hypervalent Iodines: Active Players in Asymmetric Synthesis. *Chem. Rev.* **2019**, *119*, 12033−12088.
(21) Farid, U.; Malmedy, F.; Claveau, R.; Albers, L.; Wirth, T. Stereoselective Rearrangements with Chiral Hypervalent Iodine Reagents. *Angew. Chem., Int. Ed.* **2013**, *52*, 7018−7022.
(22) Brown, M.; Kumar, R.; Rehbein, J.; Wirth, T. Enantioselective Oxidative Rearrangements with Chiral Hypervalent Iodine Reagents. *Chem. - Eur. J.* **2016**, *22*, 4030−4035.
(23) Shimogaki, M.; Fujita, M.; Sugimura, T. Metal-Free Enantioselective Oxidative Arylation of Alkenes: Hypervalent-Iodine-Promoted Oxidative C−C Bond Formation. *Angew. Chem., Int. Ed.* **2016**, *55*, 15797−15801.
(24) Hirt, U. H.; Spingler, B.; Wirth, T. New Chiral Hypervalent Iodine Compounds in Asymmetric Synthesis. *J. Org. Chem.* **1998**, *63*, 7674−7679.
(25) Dohi, T.; Maruyama, A.; Takenaga, N.; Senami, K.; Minamitsuji, Y.; Fujioka, H.; Caemmerer, S. B.; Kita, Y. A Chiral Hypervalent Iodine(III) Reagent for Enantioselective Dearomatization of Phenols. *Angew. Chem., Int. Ed.* **2008**, *47*, 3787−3790.
(26) Uyanik, M.; Yasui, T.; Ishihara, K. Enantioselective Kita Oxidative Spirolactonization Catalyzed by In Situ Generated Chiral Hypervalent Iodine(III) Species. *Angew. Chem., Int. Ed.* **2010**, *49*, 2175−2177.
(27) Haubenreisser, S.; Wöste, T. H.; Martínez, C.; Ishihara, K.; Muñiz, K. Structurally Defined Molecular Hypervalent Iodine Catalysts for Intermolecular Enantioselective Reactions. *Angew. Chem., Int. Ed.* **2016**, *55*, 413−417.
(28) Hashimoto, T.; Shimazaki, Y.; Omatsu, Y.; Maruoka, K. Indanol-Based Chiral Organoiodine Catalysts for Enantioselective Hydrative Dearomatization. *Angew. Chem., Int. Ed.* **2018**, *57*, 7200−7204.
(29) Farid, U.; Wirth, T. Highly Stereoselective Metal-Free Oxyaminations Using Chiral Hypervalent Iodine Reagents. *Angew. Chem., Int. Ed.* **2012**, *51*, 3462−3465.
(30) Muñiz, K.; Barreiro, L.; Romero, R. M.; Martínez, C. Catalytic Asymmetric Diamination of Styrenes. *J. Am. Chem. Soc.* **2017**, *139*, 4354−4357.
(31) Kitamura, T.; Muta, K.; Oyamada, J. Hypervalent Iodine-Mediated Fluorination of Styrene Derivatives: Stoichiometric and Catalytic Transformation to 2,2-Difluoroethylarenes. *J. Org. Chem.* **2015**, *80*, 10431−10436.
(32) Banik, S. M.; Medley, J. W.; Jacobsen, E. N. Catalytic, Diastereoselective 1,2-Difluorination of Alkenes. *J. Am. Chem. Soc.* **2016**, *138*, 5000−5003.
(33) Molnár, I. G.; Gilmour, R. Catalytic Difluorination of Olefins. *J. Am. Chem. Soc.* **2016**, *138*, 5004−5007.
(34) Kong, W.; Feige, P.; de Haro, T.; Nevado, C. Regio- and Enantioselective Aminofluorination of Alkenes. *Angew. Chem., Int. Ed.* **2013**, *52*, 2469−2473.
(35) Suzuki, S.; Kamo, T.; Fukushi, K.; Hiramatsu, T.; Tokunaga, E.; Dohi, T.; Kita, Y.; Shibata, N. Iodoarene-catalyzed fluorination and aminofluorination by an Ar-I/HF·pyridine/mCPBA system. *Chem. Sci.* **2014**, *5*, 2754−2760.
(36) Banik, S. M.; Medley, J. W.; Jacobsen, E. N. Catalytic, asymmetric difluorination of alkenes to generate difluoromethylated stereocenters. *Science* **2016**, *353*, 51−54.
(37) Haj, M. K.; Banik, S. M.; Jacobsen, E. N. Catalytic, Enantioselective 1,2-Difluorination of Cinnamamides. *Org. Lett.* **2019**, *21*, 4919−4923.
(38) Mennie, K. M.; Banik, S. M.; Reichert, E. C.; Jacobsen, E. N. Catalytic Diastereo- and Enantioselective Fluoroamination of Alkenes. *J. Am. Chem. Soc.* **2018**, *140*, 4797−4802.
(39) Woerly, E. M.; Banik, S. M.; Jacobsen, E. N. Enantioselective, Catalytic Fluorolactonization Reactions with a Nucleophilic Fluoride Source. *J. Am. Chem. Soc.* **2016**, *138*, 13858−13861.
(40) Sharma, H.; Mennie, K. M.; Kwan, E. E.; Jacobsen, E. N. Enantioselective Aryl-Iodide-Catalyzed Wagner−Meerwein Rearrangements. *J. Am. Chem. Soc.* **2020**, *142*, 16090−16096.
(41) Wolstenhulme, J. R.; Gouverneur, V. Asymmetric Fluorocyclizations of Alkenes. *Acc. Chem. Res.* **2014**, *47*, 3560−3570.
(42) Lozano, O.; Blessley, G.; Martinez del Campo, T.; Thompson, A. L.; Giuffredi, G. T.; Bettati, M.; Walker, M.; Borman, R.; Gouverneur, V. Organocatalyzed Enantioselective Fluorocyclizations. *Angew. Chem., Int. Ed.* **2011**, *50*, 8105−8109.
(43) Wolstenhulme, J. R.; Rosenqvist, J.; Lozano, O.; Ilupeju, J.; Wurz, N.; Engle, K. M.; Pidgeon, G. W.; Moore, P. R.; Sandford, G.; Gouverneur, V. Asymmetric Electrophilic Fluorocyclization with Carbon Nucleophiles. *Angew. Chem., Int. Ed.* **2013**, *52*, 9796−9800.
(44) Rauniyar, V.; Lackner, A. D.; Hamilton, G. L.; Toste, F. D. Asymmetric Electrophilic Fluorination Using an Anionic Chiral Phase-Transfer. *Science* **2011**, *334*, 1681−1684.
(45) Shunatona, H. P.; Früh, N.; Wang, Y.-M.; Rauniyar, V.; Toste, F. D. Enantioselective Fluoroamination: 1,4-Addition to Conjugated Dienes Using Anionic Phase-Transfer Catalysis. *Angew. Chem., Int. Ed.* **2013**, *52*, 7724−7727.
(46) Liu, J.; Yuan, Q.; Toste, F. D.; Sigman, M. S. Enantioselective construction of remote tertiary carbon−fluorine bonds. *Nat. Chem.* **2019**, *11*, 710−715.
(47) Egami, H.; Niwa, T.; Sato, H.; Hotta, R.; Rouno, D.; Kawato, Y.; Hamashima, Y. Dianionic Phase-Transfer Catalyst for Asymmetric Fluoro-cyclization. *J. Am. Chem. Soc.* **2018**, *140*, 2785−2788.
(48) Brandes, S.; Niess, B.; Bella, M.; Prieto, A.; Overgaard, J.; Jørgensen, K. A. Non-Biaryl Atropisomers in Organocatalysis. *Chem. - Eur. J.* **2006**, *12*, 6039−6052.
(49) Xu, J.; Hu, Y.; Huang, D.; Wang, K.-H.; Xu, C.; Niu, T. Thiourea-Catalyzed Enantioselective Fluorination of β-Keto Esters, AsymF. *Adv. Synth. Catal.* **2012**, *354*, 515−526.
(50) Yang, X.; Phipps, R. J.; Toste, F. D. Asymmetric Fluorination of α-Branched Cyclohexanones Enabled by a Combination of Chiral Anion Phase-Transfer Catalysis and Enamine Catalysis using Protected Amino Acids. *J. Am. Chem. Soc.* **2014**, *136*, 5225−5228.
(51) You, Y. e.; Zhang, L.; Luo, S. Reagent-controlled enantioselectivity switch for the asymmetric fluorination of β-

ketocarbonyls by chiral primary amine catalysis. *Chem. Sci.* **2017**, *8*, 621−626.
(52) Pluta, R.; Krach, P. E.; Cavallo, L.; Falivene, L.; Rueping, M. Metal-Free Catalytic Asymmetric Fluorination of Keto Esters Using a Combination of Hydrogen Fluoride (HF) and Oxidant: Experiment and Computation. *ACS Catal.* **2018**, *8*, 2582−2588.
(53) Wang, Y.; Yuan, H.; Lu, H.; Zheng, W.-H. Development of Planar Chiral Iodoarenes Based on [2.2]Paracyclophane and Their Application in Catalytic Enantioselective Fluorination of β-Ketoesters. *Org. Lett.* **2018**, *20*, 2555−2558.
(54) Levin, M. D.; Ovian, J. M.; Read, J. A.; Sigman, M. S.; Jacobsen, E. N. Catalytic Enantioselective Synthesis of Difluorinated Alkyl Bromides. *J. Am. Chem. Soc.* **2020**, *142*, 14831−14837.
(55) Cortes Gonzalez, M. A.; Nordeman, P.; Bermejo Gomez, A.; Meyer, D. N.; Antoni, G.; Schou, M.; Szabó, K. J. [18F]Fluorobenziodoxole: A no-carrier-added electrophilic fluorinating reagent. Rapid, simple radiosynthesis, purification and application for fluorine-18 labelling. *Chem. Commun.* **2018**, *54*, 4286−4289.
(56) Sarie, J.; Thiehoff, C.; Neufeld, J.; Daniliuc, C.; Gilmour, R. Enantioselective Synthesis of 3-Fluorochromanes via I(I)/I(III) Catalysis. *Angew. Chem., Int. Ed.* **2020**, *59*, 15069−15075.
(57) Geary, G. C.; Hope, E. G.; Stuart, A. M. Intramolecular Fluorocyclizations of Unsaturated Carboxylic Acids with a Stable Hypervalent Fluoroiodane Reagent. *Angew. Chem., Int. Ed.* **2015**, *54*, 14911−14914.
(58) Ulmer, A.; Brunner, C.; Arnold, A. M.; Pöthig, A.; Gulder, T. A Fluorination/Aryl Migration/Cyclization Cascade for the Metal-free Synthesis of Fluoro Benzoxazepines. *Chem. - Eur. J.* **2016**, *22*, 3660−3664.
(59) Andries-Ulmer, A.; Brunner, C.; Rehbein, J.; Gulder, T. Fluorine as a Traceless Directing Group for the Regiodivergent Synthesis of Indoles and Tryptophans. *J. Am. Chem. Soc.* **2018**, *140*, 13034−13041.
(60) Scheidt, F.; Schäfer, M.; Sarie, J. C.; Daniliuc, C. G.; Molloy, J. J.; Gilmour, R. Enantioselective, Catalytic Vicinal Difluorination of Alkenes. *Angew. Chem., Int. Ed.* **2018**, *57*, 16431−16435.
(61) Ilchenko, N. O.; Tasch, B. O. A.; Szabó, K. J. Mild Silver-Mediated Geminal Difluorination of Styrenes using an Air- and Moisture-Stable Fluoroiodane Reagent. *Angew. Chem., Int. Ed.* **2014**, *53*, 12897−12901.
(62) Zhou, B.; Haj, M. K.; Jacobsen, E. N.; Houk, K. N.; Xue, X.-S. Mechanism and Origins of Chemo- and Stereoselectivities of Aryl Iodide-Catalyzed Asymmetric Difluorinations of β-Substituted Styrenes. *J. Am. Chem. Soc.* **2018**, *140*, 15206−15218.
(63) Scheidt, F.; Neufeld, J.; Schäfer, M.; Thiehoff, C.; Gilmour, R. Catalytic Geminal Difluorination of Styrenes for the Construction of Fluorine-rich Bioisosteres. *Org. Lett.* **2018**, *20*, 8073−8076.
(64) Beesley, R. M.; Ingold, C. K.; Thorpe, J. F. CXIX.—The formation and stability of spiro-compounds. Part I. spiro-Compounds from cyclohexane. *J. Chem. Soc., Trans.* **1915**, *107*, 1080−1106.
(65) Wodrich, M. D.; Wannere, C. S.; Mo, Y.; Jarowski, P. D.; Houk, K. N.; Schleyer, P. v. R. The Concept of Protobranching and Its Many Paradigm Shifting Implications for Energy Evaluations. *Chem. - Eur. J.* **2007**, *13*, 7731−7744.
(66) Lee, C.; Yang, W.; Parr, R. G. Development of the Colle-Salvetti correlation-energy formula into a functional of the electron density. *Phys. Rev. B: Condens. Matter Mater. Phys.* **1988**, *37*, 785−789.
(67) Becke, A. D. Density-functional Thermochemistry. III. The Role of Exact Exchange. *J. Chem. Phys.* **1993**, *98*, 5648−5652.
(68) Grimme, S.; Antony, J.; Ehrlich, S.; Krieg, H. A consistent and accurate ab initio parametrization of density functional dispersion correction (DFT-D) for the 94 elements H-Pu. *J. Chem. Phys.* **2010**, *132*, 154104−154119.
(69) Grimme, S.; Ehrlich, S.; Goerigk, L. Effect of the damping function in dispersion corrected density functional theory. *J. Comput. Chem.* **2011**, *32*, 1456−1465.
(70) Marenich, A. V.; Cramer, C. J.; Truhlar, D. G. Universal Solvation Model Based on Solute Electron Density and on a Continuum Model of the Solvent Defined by the Bulk Dielectric Constant and Atomic Surface Tensions. *J. Phys. Chem. B* **2009**, *113*, 6378−6396.
(71) Arrica, M. A.; Wirth, T. Fluorinations of α-Seleno Carboxylic Acid Derivatives with Hypervalent (Difluoroiodo)toluene. *Eur. J. Org. Chem.* **2005**, *2005*, 395−403.
(72) Kitamura, T.; Kuriki, S.; Morshed, M. H.; Hori, Y. A Practical and Convenient Fluorination of 1,3-Dicarbonyl Compounds Using Aqueous HF in the Presence of Iodosylbenzene. *Org. Lett.* **2011**, *13*, 2392−2394.
(73) Kitamura, T.; Muta, K.; Kuriki, S. Catalytic fluorination of 1,3-dicarbonyl compounds using iodoarene catalysts. *Tetrahedron Lett.* **2013**, *54*, 6118−6120.

https://dx.doi.org/10.1021/jacs.0c09323
J. Am. Chem. Soc. 2020, 142, 20048−20057